An Integrated Approach to Assess Water Quality of the Karnaphuli Estuary through Nutrient Dynamics during the Dry Season

Adiba Mosharraf[1], Ferdousi Begum[2*], Farhana Akter[2], Modhuparna Dey[3] and Md. Abu Bin Hasan Susan[4]

[1]Climate Change and Environment Unit, Institute of Water Modelling, Uttara, Dhaka-1230, Bangladesh
[2]Department of Chemistry, Bangladesh Maritime University, Pallabi Mirpur-12, Dhaka-1216, Bangladesh
[3]Department of Marine Fisheries and Aquaculture, Bangladesh Maritime University, Pallabi Mirpur-12, Dhaka-1216, Bangladesh
[4]Department of Chemistry, University of Dhaka, Dhaka-1200, Bangladesh

Manuscript received: 02 November 2025; accepted for publication: 16 July 2026

ABSTRACT: The Karnaphuli River, one of the largest and most active rivers of Bangladesh, has historically served as a hub for numerous human activities such as port operations, shipping, and other operations. Numerous industrial plants, welding businesses, fertilizer firms, and multiple oil industries are all located along the riverbank. Thus, the water quality of this river is deteriorating as a result of pollutants being directly released into water bodies. Here, the contamination status of surface water (SW) collected from 10 stations within the Karnaphuli estuary (KE) in the dry season of 2023 was investigated. A comprehensive assessment was conducted using widely applied nutrient-related water quality indices, including the Nitrogen-Phosphorus Index (NPI), Trophic State Index (TRIX), and Carlson Trophic State Index (CTSI), derived from measured physicochemical parameters such as temperature, salinity, pH, turbidity, electrical conductivity (EC), density, dissolved oxygen (DO), and total dissolved solids (TDS), along with concentration of nutrients (phosphate, nitrate, nitrite, ammonia, and silicate) and chlorophyll-*a*. The results indicate that the quality of SW was generally *qualified* according to NPI, while TRIX and CTSI suggest predominantly *oligotrophic* to *mesotrophic* conditions, with localized variations across stations. Pearson correlation analysis revealed significant relationships among salinity-driven parameters and nutrient-biological interactions. Exploratory multivariate analyses (principal component analysis and hierarchical cluster analysis), supported by spatial distribution patterns, suggest possible influences of estuarine mixing processes and nearby anthropogenic activities on water quality variability, although direct source attribution requires further investigation.

Keywords: Pearson Correlation; Eutrophication; Karnaphuli Estuary; Nutrients; Chlorophyll-a

INTRODUCTION

Among the most prominent estuaries in Bangladesh, Karnaphuli is situated on the eastern south side of the country. This dynamic ecosystem plays a vital role, serving as a crucial transportation hub, a haven for fishing communities, a home to docking yards, and a source of fresh water for commercial use (Siddique & Akter, 2012). The intricate network of tidal canals and mudflats of Karnaphuli provides a vital breeding ground and nursery for a multitude of fish species, crabs, and other aquatic creatures. The ecosystem of this estuary is shaped by seasonal variations and anthropogenic impacts and remains critical for biodiversity and the local economy (Mosharraf et al., 2026). Additionally, the nutrient-rich water of the estuary nurtures a diverse food web, making it a sanctuary for both marine and avian life. This rich tapestry of life is a testament to the immense ecological significance of the Karnaphuli estuary (KE).

Nutrient enrichment in coastal and estuarine systems typically follows a sequential pathway: anthropogenic nutrient inputs from agricultural fertilizers, wastewater discharge, and urban runoff initially stimulate primary production, leading to increased phytoplankton biomass and enhanced organic matter (OM) supply to the food web (Nixon, 1995; Howarth and Marino, 2006). This OM fuels coastal food webs that support diverse fisheries, representing an initial positive ecological response to nutrient availability. However, when nutrient loading exceeds the assimilative capacity of the ecosystem, the system transitions toward eutrophication, defined as an increase in the rate of OM supply to the ecosystem (Nixon, 1995). The subsequent degradation pathway involves excessive phytoplankton

Corresponding Author: Ferdousi Begum
Email: ferdousi.chem@bmu.edu.bd

DOI: https://doi.org/10.3329/dujees.v15i1.91983

and macroalgal growth, including harmful algal blooms; reduced light penetration and loss of submerged aquatic vegetation; sinking of ungrazed algal biomass to bottom waters; microbial decomposition consuming dissolved oxygen (DO); and development of hypoxic or anoxic conditions when oxygen consumption exceeds resupply, particularly in stratified systems (CENR, 2000; Rabalais et al., 2010). These biogeochemical feedbacks can further alter nutrient cycles, potentially accelerating eutrophication through sediment phosphorus release and changes in nitrogen transformation pathways (Paerl, 2006). While nitrogen is often the primary driver of coastal eutrophication, both nitrogen and phosphorus reductions are necessary for effective management, as an imbalanced nitrogen-phosphorus ratio can shift phytoplankton community composition toward harmful species (Paerl, 2006). In the KE, nutrient inputs from industrial effluents, port operations, and urban drainage may initiate this enrichment cascade, though the specific trajectory depends on physical factors such as flushing rate and stratification, and biological responses, including grazing pressure and algal community structure, which require further investigation.

A comprehensive evaluation of the KE is essential to understand the biological and environmental implications of nutrient enrichment. In coastal and estuarine ecosystems, increasing attention has been given to the sources, dynamics, and spatiotemporal variability of nutrient accumulation, as these processes are closely linked to ecological disturbances such as algal blooms, eutrophication, and hypoxia (Wang et al., 2012; Sun et al., 2017). In the context of the Karnaphuli River (KR), previous studies indicate a rising trend of pollution driven by rapid industrialization, urban expansion, and population growth in the Chattagram region, with untreated wastewater discharge and industrial effluents identified as major contributors (Karim et al., 2018; Uddin et al., 2020). Such inputs pose significant risks to aquatic life and estuarine water quality if not effectively managed. However, it is important to note that the present study is based on a single-month reconnaissance survey (February 2023), which limits the ability to establish temporal trends or definitively confirm increasing pollution levels. Therefore, the primary objective of this study was to investigate the physicochemical characteristics, including temperature, pH, electrical conductivity (EC), salinity, total dissolved solids (TDS), DO, density, and turbidity, alongside the spatial variability and distribution of concentration of nutrients and chlorophyll-*a* (chl-*a*) in surface water (SW) of the KE during the dry season. To achieve this, nutrient contamination and trophic conditions were evaluated using the Nitrogen-Phosphorus Index (NPI), Trophic State Index (TRIX), and Carlson Trophic State Index (CTSI). Pearson correlation analysis, principal component analysis (PCA), and hierarchical cluster analysis (HCA) were complemented to explore potential pollution sources for the study period, as well as Inverse Distance Weighted (IDW) interpolation for spatial visualization. While earlier studies, such as Uddin et al. (2020), provided seasonal baseline data and Sadi et al. (2024) focused on specific pollution indicators, no prior research has integrated NPI, TRIX, and CTSI with multivariate statistical techniques and geospatial interpolation to evaluate nutrient-driven trophic status in the KE. Moreover, inconsistencies among trophic classifications (e.g., *oligotrophic*, *mesotrophic*, and *eutrophic*) have not been systematically examined within this estuarine context. This study addresses these gaps by (i) applying multiple trophic indices to a single dataset, (ii) interpreting discrepancies among indices through physicochemical linkages, and (iii) integrating PCA, HCA, and inverse distance weighted (IDW) approaches for improved identification of potential pollution sources and spatial patterns. The findings provide a valuable baseline snapshot of nutrient dynamics in the KE, contributing to future monitoring efforts, supporting Sustainable Development Goal 14 (SDG 14), and informing targeted conservation and management strategies, while emphasizing the need for long-term studies to validate temporal patterns and ensure sustainable ecosystem health.

MATERIALS AND METHODS

Study Area and Sample Collections

The KR, the primary river in Chattagram, originates in the Lushai Hills of Mizoram, India, and flows ~ 270 km south and southwest through southeastern Bangladesh to the Bay of Bengal (BoB). As a tidal river with semi-diurnal characteristics, flood flows extend far upstream in the Halda River and approach Kaptai Dam (Karim et al., 2018; Alam and Matin, 2014; Mosharraf et al., 2026). In this study, SW samples of the downstream of the KR were collected from 10 stations at around 1.5 km intervals using a water sampler during February 2023. Sampling was conducted during low tidal stage (slack water, around 1-2 hours after low tide) between 09:00

and 11:00 am local time to minimize tidal variability and ensure consistency across stations. Samples were collected from 0.5 m below the water surface at each station to represent the well-mixed surface layer. Sampling locations were determined using a global positioning system (GPS). Sample station occupies an area between latitude 22°18’60” N and 22°12’32” N and longitude 91°48’51” E and 91°48’11” E. Fig. 1 and Table 1 show the geographical coordinates of all sampling stations from which SW was collected from the KE. Sample bottles were sealed airtight, stored in an adiabatic ice box at 4 °C, and sterilized with H_2SO_4 for further study.

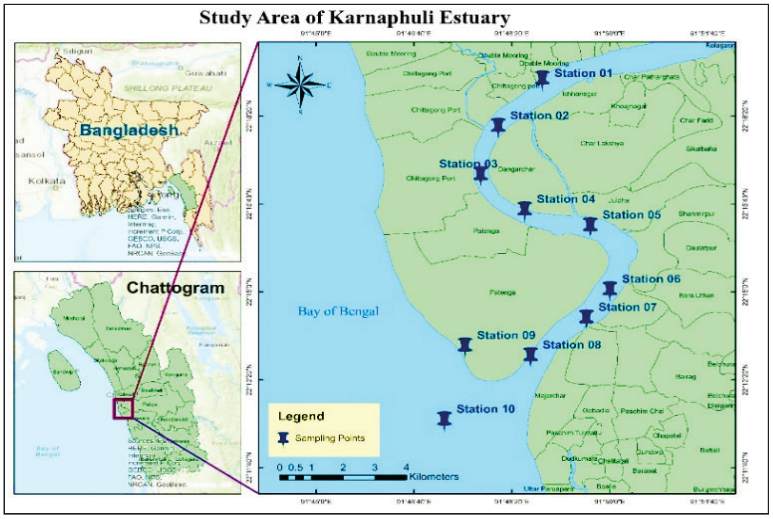

Figure 1: Geographical Coordinates of all the Sampling Stations of the KE. (Satellite View of Bangladesh and Chattagram with its Adjacent Neighbors (Left Panel) and Sampling Stations from which SW was Collected (Right Panel). The Stations are Numbered to Maintain their Sampling Times, and Sampling Sites are Colored Orange. Stations 1–4 Represent the Upper Estuary (Low Salinity, River-Dominated), Stations 5–8 Represent the Middle Estuary (Brackish, Mixing Zone), and Stations 9–10 Represent the Lower Estuary (Marine-Influenced). Sampling Locations were Determined Using GPS (see Table 1 for Coordinates)

Table 1: Description of the Sampling Points in the KE

St No.	Latitude	Longitude	Local Name
1.	22°19’00”	91°48’51”	Near Karnaphuli Dockyard
2.	22°18’06”	91°48’06”	Near Chattagram Port
3.	22°17’11”	91°47’48”	Near Dangar Char
4.	22°16’31”	91°48’33”	9 No. Ghat
5.	22°16’13”	91°49’40”	Near Chattagram Boat Club
6.	22°15’01”	91°50’00”	Near Anowara
7.	22°14’28”	91°49’36”	Near Bangladesh Marine Academy
8.	22°13’45”	91°48’39”	Near Naval Academy
9.	22°13’56”	91°47’32”	Patenga Sea Beach
10.	22°12’32”	91°48’11”	Near Parki Beach

Assessment of Physicochemical Parameters

Water quality of SW of the KE was considered by evaluating 10 physicochemical properties, where temperature, salinity, pH, EC, TDS, and DO were determined in situ using a WTW inoLab Multi 9310 IDS multiparameter probe via electrometric methods. Density was measured with an Anton Paar DMA 4500 ME vibrating U-tube density meter. Turbidity was quantified using an EPA-compliant HI88703 benchtop turbidity meter (HANNA Instruments) based on the nephelometric method.

Analysis of Concentration of Nutrient

Nutrient concentrations in SW samples were determined using a HACH DR 3900 single-beam UV-visible spectrophotometer (Sakib et al., 2025). Concentration of phosphate, nitrate, nitrite, and silicate were quantified following HACH Powder Pillow Methods 8048, 8171, 8507, and 8185, respectively, where ammonia was measured using the HACH Nessler Method 8038.

Analysis of Concentration of Chlorophyll-*a*

Chl-*a* was determined following a standard spectrophotometric method after pigment extraction. A known volume of water (filtered in 50 mL increments, depending on phytoplankton density) was passed through a 47 mm, 0.45 µm pore size nitrocellulose membrane filter under low-light conditions to prevent pigment degradation. The retained algal material on the filter was transferred into a pre-labeled test tube, and pigments were extracted using 5 mL of 90 % acetone solution. The samples were tightly capped, vortexed, and kept in dark conditions for approximately 24 hours at low temperature (freezer conditions) to ensure complete extraction. Following extraction, the samples were centrifuged for 15 minutes (~ 500 rpm) to obtain a clear supernatant, which was carefully transferred into a 1-inch path length glass cuvette for analysis. Blank correction was performed using acetone blanks (prepared with 5 mL of acetone and a clean filter without pigments) to eliminate background absorbance. Absorbance (optical density) was then measured at wavelengths of 750, 664, 647, 630, and 600 nm using a spectrophotometer, and the corrected values were applied to standard equations to determine Chl-*a* concentration. Subtract the absorbance at 750 nm from the 630, 647, and 664 nm values (turbidity correction). The following equation was proposed by Jeffrey and Humphrey (1975) to calculate the concentration of chl-*a*.

$$mg\ Chl - \frac{a}{L} = \frac{\text{S [11.85 (Abs664) − 1.54 (Abs647)− 0.08 (Abs630)]}}{V} \ldots \text{(i)}$$

Where S = The volume of acetone used for the extraction (mL); V = The volume of water filtered (L); L = The cell path length (cm).

Water Quality Indices

Nitrogen-Phosphorus Index

Total nitrogen (cumulative of nitrate, nitrite, and ammonia) as well as total phosphate are the foremost contributors that affect the quality of the aquatic component. Thus, the index is calculated as follows:

$$NPI = \frac{1}{2}\left(\frac{TPi}{TPs} + \frac{TNi}{TNs}\right) \ldots\ldots\ldots \text{(ii)}$$

Where, TPi = measured value of total phosphate, TPs = standard value of total phosphate, TNi = measured value of total nitrogen, TNs = standard value of total nitrogen. The value classified as NPI ≤ 1 is *qualified*, 1< NPI ≤ 2 for *moderate*, and NPI > 2 for *bad* water quality (Zhang and Liu 2021).

Trophic Index

TRIX is fundamental to ecosystem structure and inextricably tied to biotic integrity and water quality. Four parameters are used (Vollenweider et al.,1998) to calculate the TRIX and the index is scaled from 0-4, 4-5, 5-6, and 6-10, for the water quality categorized as *high, good, moderate, poor,* and *degraded*, respectively, which are marked as *oligotrophic*, *mesotrophic*, *eutrophic*, and *hypertrophic*, respectively (Pettine et al., 2007; Vollenweider et al., 1998). The index is calculated as follows:

$$TRIX = \frac{1}{1.2}[\log(M_{chl-a} M_{DO} M_{TIN} M_{TP}) + 1.5] \ldots \text{(iii)}$$

Here, TP (total phosphate) = dissolve inorganic phosphate, TIN (total inorganic nitrogen) = dissolve inorganic nitrate + dissolve inorganic ammonia + dissolved inorganic nitrite, %DO = oxygen saturation, measured from the following equation:

$$\%DO = \frac{100 \times DO(\frac{mg}{L})}{8.8044} \ldots\ldots\ldots \text{(iv)}$$

Carlson Trophic State Index

Trophic state (the whole bulk of biomass in a given water body) and trophic state index (*TSI*) are considered via measured total phosphate (*TP*), concentration of chl-*a*, and secchi disc transparency (*SDT*) (Ayoade et al., 2019; Carlson, 1977). The equation is followed by several steps: TSI (Chl-*a*) = 9.81ln (Chl-*a*) + 30.6; TSI (*TP*) = 14.42 ln (TP) + 4.15; TSI (*SDT*) = 60 - 14.41 ln (SD); where *TP* = total phosphorus; Chl-*a* = concentration of chl-*a* (µg/L); *SDT* = Secchi disc transparency (m); The calculation for Secchi disk depth: (Baughman et al., 2015) $Secchi\ disk = 9.4109x^{-1.243}$, where, turbidity in NTU. The final equation of CTSI is given in equation (v)

$$CTSI = \frac{TSI(TP)+TSI(SDT)+TSI(Chl-a)}{3} \ldots\ldots \text{(v)}$$

However, TSI is classified as 0 - 40, 40 - 50, 50 - 80, and 80 - 100 for *oligotrophic*, *mesotrophic*, *eutrophic*, and *hypertrophic* conditions of water, respectively (Carlson 1977).

Spatial Analysis and Statistical Analysis

IDW interpolation, a deterministic mathematical method, was employed to visualize the spatial distribution of variables across the KE, recognizing the greater influence of closer known values (GIS Geography, 2021). Pearson correlation assessed the interrelationships between physicochemical properties, nutrients, and chl-*a*. To identify pollution sources related to human activities, PCA was utilized (Rezaei and Sayadi, 2014). HCA, known for providing intuitive similarity correlations and visual summaries via dendrograms, was used to explore relationships within the complete dataset (Bruce et al., 2020). ArcGIS 10.8, Jupyter Notebook v6.0.3, Microsoft Excel, and R version 3.6.3 facilitated these analyses.

Land Use and Land Cover Analysis

To assess the present land use and land cover (LULC) conditions surrounding the KE, the ESA WorldCover 10 m v200 dataset was utilized. This global product provides a 10 m resolution land cover map from 2021. For the purposes of this study, the dataset was reclassified in Google Earth Engine (GEE) into four major categories: built-up, vegetation, bare soil, and water body, following the classification scheme of Zanaga et al. (2022).

RESULTS AND DISCUSSION

Water Quality Parameters: Physicochemical Properties, Concentration of Nutrients, and Chlorophyll-*a* of Surface Water

Figures 2 and 3 represent the distributions of physicochemical parameters and concentration of nutrients with chl-*a* across the 10 sampling stations respectively. Temperature remained relatively stable (24.5-25.7 °C, mean 24.9±0.3743 °C), reflecting the cool, dry climatic conditions of February. Salinity exhibited a clear seaward gradient (4.39-15.8 ppt), increasing toward Station 10 as freshwater mixing diminished, consistent with the estuarine transition zone. pH ranged from 7.87 to 8.45 (mean 8.03±0.1858), typical of brackish water influenced by marine buffering. DO (3.2-7.9 mg/L, mean 4.79±1.5737 mg/L) fell marginally below the ECR (2023) (Table 2), likely reflecting elevated biochemical oxygen demand from OM decomposition, light-limited photosynthesis due to high turbidity, and reduced atmospheric reaeration under stratified conditions. Turbidity varied markedly across stations (20.2-842 NTU, mean 189.04±247.3340 NTU). Station 9 (Patenga Sea Beach) recorded the highest turbidity (842 NTU), which far exceeds the DoPHE (2019) guideline of 10 NTU and the WHO (2007) range of 5-25 NTU. This extreme value at the marine-influenced station likely reflects wave-driven sediment resuspension at the beach interface, localized bottom disturbance from port and fishing vessel activities. TDS (3.86-12.6 mg/L) and EC (7.72-25.20 µS/cm) tracked salinity patterns, while density (1.0013-1.0131 g/cm^3) mirrored the freshwater-marine mixing gradient.

Nutrient distributions (Fig. 3) revealed phosphate enrichment across all stations (0.12-0.75 mg/L), with most values exceeding the ECR guideline (Table 2). Nitrate (0.3-0.8 mg/L) and nitrite (0.004-0.012 mg/L) occurred at comparatively lower concentrations. Ammonia displayed the widest range (0.02-4.16 mg/L, mean 0.734±1.2919 mg/L), with Station 9 recording a pronounced maximum that far surpassed the ECR limit (Table 2); this spatial pattern implicates localized anthropogenic inputs such as untreated sewage, industrial effluent, or organic waste decomposition. Silicate varied from 2.2 to 11.1 mg/L, with higher values at upstream stations consistent with freshwater delivery from weathering sources. *Chl-a* concentrations (0.00117-0.00745 mg/L, mean 0.00383±0.00219 mg/L), when converted to standard units, indicated mesotrophic to eutrophic conditions according to DoPHE criteria, with elevated values at nutrient-enriched stations suggesting stimulated phytoplankton productivity.

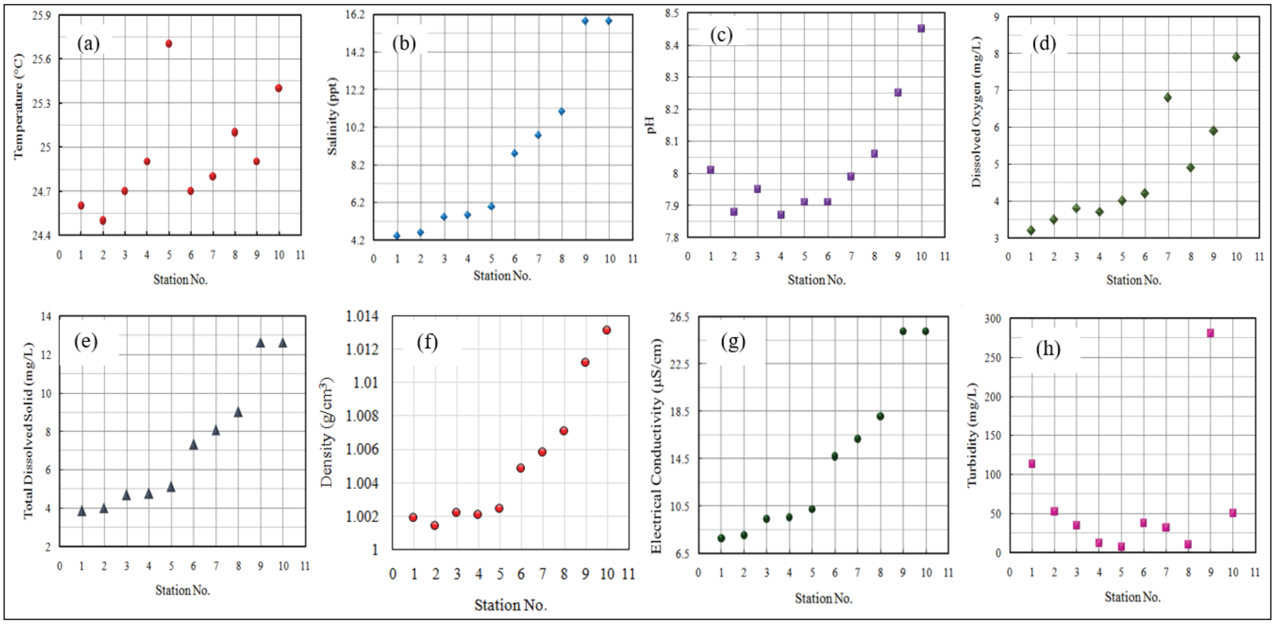

Figure 2: Physicochemical Parameters, (a) Temperature, (b) Salinity, (c) pH, (d) DO, (e) TDS, (f) EC, (g) Turbidity, and (h) Density of SW Collected from the KE

Table 2 summarizes the statistical analysis of water quality parameters against ECR (2023) standards. While temperature, salinity, pH, and TDS remained within acceptable ranges, the collective deviations in DO, ammonia, phosphate, and turbidity indicate localized ecosystem stress. The ammonia exceedance, in particular, signals active nitrogen loading that, coupled with elevated phosphate, creates conditions conducive to eutrophication (ATSDR, 2004). These findings highlight spatial heterogeneity driven by the freshwater-marine gradient superimposed with point-source anthropogenic inputs along the urbanized estuarine corridor.

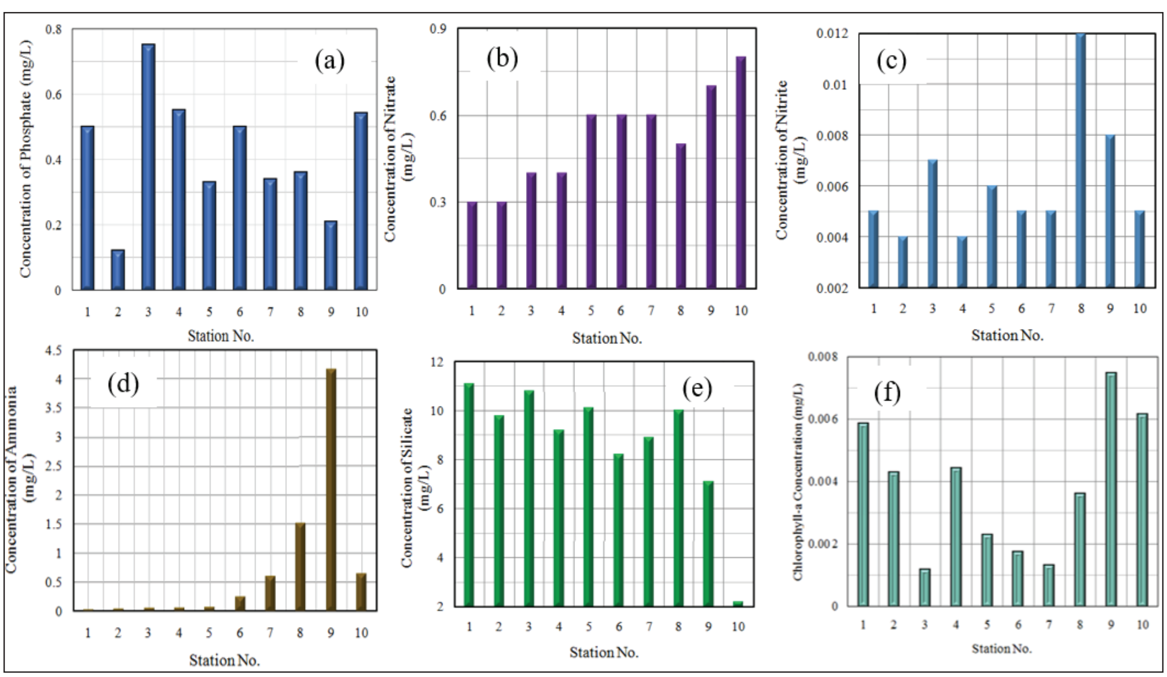

Figure 3: Concentration, (a) Phosphate, (b) Nitrate, (c) Nitrite, (d) Ammonia, (e) Silicate, and (f) Chl-*a* of SW Collected from the KE

Table 2: Mean, Maximum, Minimum, and Standard Deviation of Various Water Quality Parameters of SW Collected from the KE with Various Standards

Parameter	Mean	Max.	Min.	Std. Dev.	ECR (2023)	WHO (2007)	DoPHE (2019)
Temperature (°C)	24.93	25.7	24.5	0.3743	-	30	20 - 30
Salinity (ppt)	8.693	15.8	4.39	4.3658	-	-	5 - 18
pH	8.028	8.45	7.87	0.1858	6-9	8.5	6.5 - 8.6
DO (mg/L)	4.79	7.9	3.2	1.5737	≥ 5	< 13 - 14	6
EC (µS/cm)	14.4	25.2	7.72	6.6861	-	1.5	9 - 22.37
TDS (mg/L)	7.201	12.6	3.86	3.3422	1000	< 1.00	10
Turbidity (NTU)	189.04	842	20.2	247.3340	-	5 - 25	10
Density (g/cm^3)	1.0052	1.0131	1.0013	0.0041	-	-	-
Phosphate (mg/L)	0.42	0.75	0.12	0.1841	0.5	1	6
Nitrate (mg/L)	0.52	0.8	0.3	0.1686	7	50	10
Nitrite (mg/L)	0.0061	0.012	0.004	0.0024	-	3	< 1
Ammonia (mg/L)	0.734	4.16	0.02	1.2919	0.3	1.5	0.5
Silicate (mg/L)	8.74	11.1	2.2	2.5898	-	1	< 28
Chl-*a* (mg/L)	0.00383	0.00745	0.00117	0.00219	-	-	0.001 - 0.01

Water Quality Status of the Karnaphuli Estuary

Nitrogen Phosphorus Index

SW of the selected study area of the KE showed an average *qualified* status according to the NPI, which results in good water conditions with a low risk of nutrient pollution. A slightly higher value of NPI was observed at Station 9 (Patenga), marked as *moderate* due to an increase in concentration of ammonia (Fig. 4(a)). Artificial fertilizers are a significant source of anthropogenic nitrate and nitrite, and nitrate is also produced in the waste streams of several industrial operations. In addition, the main sources of nitrate in the environment are inorganic fertilizers and the nitrification of animal manure. Nevertheless, human waste contributions also need to be considered. Industrial wastewater, wastewater, feedlot discharges, septic systems, landfill leachate, lawn fertilizers, storm sewer overflow, nitric oxide and nitrogen dioxide from vehicle exhaust, and agricultural and urban runoff are some examples of point and non-point anthropogenic sources that may also contribute to high concentrations of ammonia in the SW of the KE.

Trophic Index

TRIX was calculated for all stations individually, and only two stations showed different water quality conditions. Station 9 (Patenga Sea Beach) and station 10 (Parki Beach) demonstrate the *mesotrophic* condition, which describes the water quality condition as *good* and the possibilities of *medium eutrophication*. However, other stations showed an *oligotrophic* condition, indicating that the level of eutrophication was low (Fig. 4(b)). *Oligotrophic* and *mesotrophic* conditions in water bodies are typically determined by the availability of nutrients and associated ecological factors. *Oligotrophic* conditions are often found in pristine or less-developed river systems, where nutrient levels are naturally low due to limited nutrient inputs. In contrast, *mesotrophic* conditions typically occur in rivers that receive a moderate number of nutrient inputs, often as a result of agricultural runoff, point source pollution, or other human activities. This transition from *oligotrophic* to *mesotrophic* conditions in rivers is commonly observed when increased nutrient inputs, nitrogen and phosphorus, result in enhanced primary production, including algal and plant growth. The specific conditions and nutrient thresholds for classifying a river as *oligotrophic* or *mesotrophic* can vary by region and depend on local environmental factors (Hawkins et al., 2000).

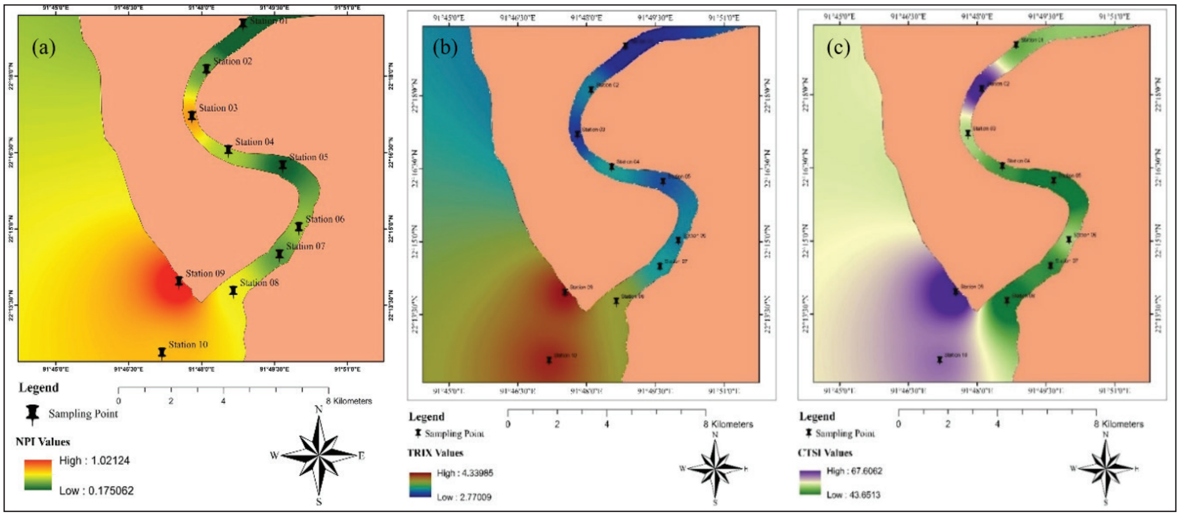

Figure 4: Spatial Distribution of (a) NPI, (b) TRIX, and (c) CTSI for SW Collected from the KE

Carlson Trophic State Index

According to CTSI, the average condition of SW of the KE was *marginal* to *mesotrophic*; thus, a moderate level of algal condition led to a fair condition. However, Stations no 1, 9, and 10 demonstrated a *eutrophic* condition, whereas the rest of the stations were marginal to this level (Fig. 4(c)). *Eutrophication* is characterized by an overabundance of nutrient-fueled algal and plant growth, which can lead to several negative ecological and water quality parameters. Including algal blooms, reduced water clarity, oxygen depletion, and deterioration of aquatic habitats. Transition from *mesotrophic* to *eutrophic* conditions in rivers is a well-documented phenomenon and often results from human activities that increase nutrient loading to the water, promoting the growth of algae and aquatic plants (Smith and Schindler, 2009).

Correlation Analysis

Pearson Correlation between Water Quality Parameters

Pearson correlation analysis revealed several statistically significant relationships (p <0.05), particularly strong positive correlations among salinity, EC, TDS, and density (r ≥0.9), indicating a dominant influence of saline water intrusion and mixing processes. Turbidity showed a significant positive correlation with the concentration of ammonia and chl-*a*, suggesting potential links to anthropogenic inputs and agriculture run-off. In contrast, the concentration of silicate exhibited significant negative correlations with salinity and related parameters, reflecting dilution effects. However, several weak correlations (p > 0.05), particularly involving phosphate and nitrite, were not considered statistically meaningful (Fig. 5).

Source Analysis of Water Quality Parameters

PCA with varimax rotation and Kaiser normalization was applied to identify potential sources of variation in water quality parameters, and only factors with eigenvalues >1 were retained (Fig. 6). The first two principal components explained 74.63 % of the total variance, with PC1 accounting for 59.22 % and PC2 for 15.41 %. Factor loadings were classified as follows: >0.70 (*extremely strong*), 0.50-0.70 (*strong*), 0.30-0.50 (*moderate*), and <0.30 (*weak*) (Howladar et al., 2020; Huang et al., 2021).

PC1 showed moderate positive loadings (>0.30) for salinity, EC, TDS, and density, with significant negative loadings on other parameters. This indicates that PC1 primarily represents EC-related properties driven by dissolved solids and salinity. These variations likely result from estuarine mixing, freshwater inflow, or evaporation processes. Thus, PC1 reflects the combined influence of ionic strength and dissolved solids on water quality. PC2 shows a strong positive relation for turbidity (>0.50) and ammonia (>0.30), provided that this component captures variability linked to water clarity and nutrient levels. A positive correlation with turbidity implies that higher turbidity (i.e., reduced water clarity) is associated with increased ammonia levels, possibly due to OM or pollution sources impacting the SW.

	Temperatu	Salinity	pH	DO	Conductivit	TDS	Turbidity	Density	Phosphate	Ammonia	Nitarte	Nitrite	Silicate	Chl-a
Temperature	1.0													
Salinity	0.4	1.0												
pH	0.4	0.9	1.0											
DO	0.4	0.9	0.8	1.0										
Conductivity	0.4	1.0	0.9	0.9	1.0									
TDS	0.4	1.0	0.9	0.9	1.0	1.0								
Turbidity	-0.2	0.5	0.5	0.2	0.5	0.5	1.0							
Density	0.4	1.0	0.9	0.9	1.0	1.0	0.4	1.0						
Phosphate	0.0	-0.2	0.0	-0.1	-0.2	-0.2	-0.3	-0.1	1.0					
Ammonia	0.1	0.7*	0.5	0.4	0.7*	0.7*	0.8*	0.7	-0.4	1.0				
Nitarte	0.6*	0.9	0.7	0.8	0.9	0.9	0.2	0.9	-0.1	0.5	1.0			
Nitrite	0.2	0.4	0.2	0.1	0.4	0.4	0.1	0.3	-0.1	0.5	0.2	1.0		
Silicate	-0.4	-0.8*	-0.8	-0.8*	-0.8*	-0.8	-0.2	-0.8	0.0	-0.3	-0.8	0.1	1.0	
Chl-a	0.1	0.4	0.6*	0.2	0.4	0.4	0.7*	0.5	-0.3	0.5	0.1	0.0	-0.4	1.0

Figure 5: Pearson Correlation Matrix Showing the Relationship between Physicochemical Properties, Concentration of Nutrients, and Chl-*a* of SW (Threshold Value of the Relation Coefficient at a 95 % Confidence Level) Collected from the KE. *Green* and *red* Colors Indicate a Strong Positive and Negative Relationship between the Parameters and the Calculated Indices. (*) Marks Indicate a Significant Correlation (p-value ≈ 0.024 (Significant))

Hierarchy Cluster Analysis

The dendrogram shown in Fig. 7 represents the results of an HCA performed on 10 stations based on their similarity or dissimilarity, likely in terms of environmental parameters or pollution levels. The vertical axis indicates the distance or dissimilarity between clusters, with lower values signifying greater similarity. Stations 6 and 7 are the most similar and cluster together first, followed by their merging with Station 5 and then Station 8. A separate cluster is formed by Stations 1, 2, 3, and 4, indicating moderate similarity among them. Stations 9 and 10 form another distinct cluster, which joins the rest only at a higher dissimilarity level, suggesting that they differ significantly from the others. The overall structure implies that the stations can be grouped into three main clusters, reflecting spatial or environmental variability across the sampled locations.

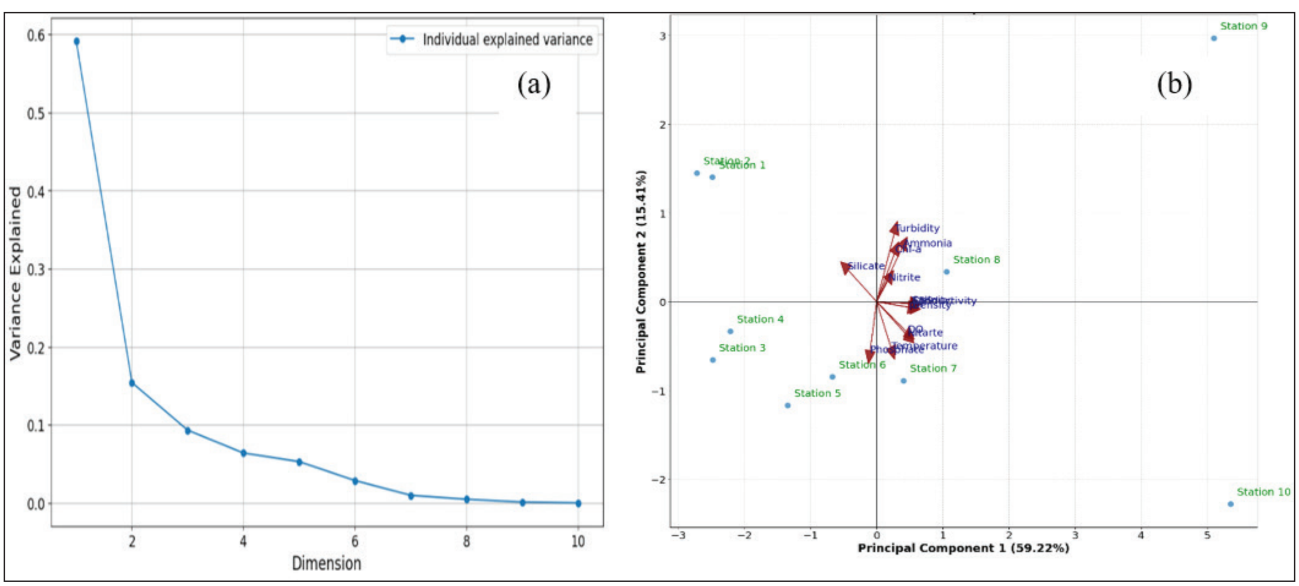

Figure 6: (a) Scree Plot and (b) Component Loading of PCA of SW of the KE

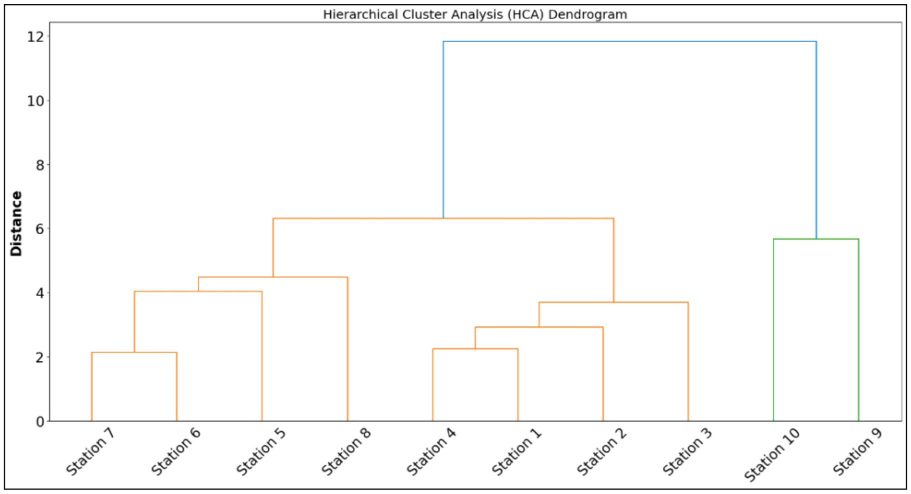

Figure 7: Cluster Analysis of the Collected SW from the KE

Land Use and Land Cover Analysis of the Karnaphuli Estuary

LULC analysis of the KE revealed a spatial distribution pattern that aligns closely with major point and non-point pollution sources surrounding the waterbody (Fig. 8 (a)). The KE is bordered by extensive built-up areas, especially across the western downstream and coastal regions, where anthropogenic pressure is highest. This spatial pattern corresponds with the high density of water-dependent industries reported by Uddin et al. (2020), who documented 1,120 water-dependent industrial units located along the KR, including major clusters at Kaloorghat (150), Chaktai (116), Fisheryghat (123), Dry-dock (143), Firingibazar (112), Sadarghat (98), Jaldia (60), and the Port area (98). Additionally, Uddin et al., (2020) identified 313 pollution-contributing industries, comprising textile (65), tanneries (25), oil refineries (5), T.S.P. (7) and urea (2) fertilizer plants, cement factories (7), chemical industries (4), detergent and soap plants (5), fish processing plants (60), and 105 other industrial units, all of which intensify the pollutant load entering the estuary, which is demonstrated in Fig. 8 (c).

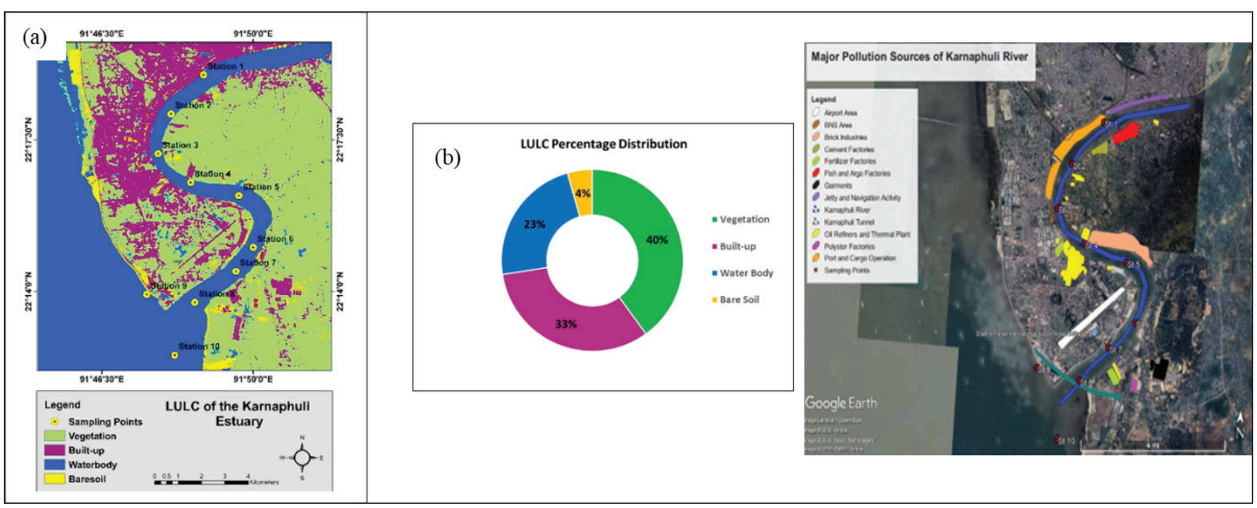

Figure 8: (a) LULC Map (b), % Distribution of LULC in KE, and (c) Field Verification of Activity along the River Bank of Both Sides of the Downstream of KE

Figure 8 (a) demonstrates that monitoring stations lie within these heavily urbanized and industrially influenced zones, particularly Stations 3, 4, and 5, where deterioration reflected by assessed indices aligns with surrounding land-use patterns. While vegetation still covers about 40 % of the landscape and provides some buffering capacity (Fig. 8 (b)), it is important to note that agricultural fields adjacent to vegetated areas may also act as sources of nutrient contamination due to fertilizer runoff, counteracting part of this natural buffering effect. With the estuary itself occupying 23 % of the area and directly receiving runoff from these mixed land-use types, the system remains highly vulnerable.

LIMITATION OF THE STUDY

The assessment of the surface water quality of the KE is based on a single sampling campaign conducted in February 2023, providing only a snapshot of estuarine conditions and therefore not accounting for seasonal or interannual variability in water quality. In addition, the relatively limited number of sampling stations (n = 10) may constrain the spatial representativeness and the robustness of multivariate analyses such as PCA and HCA. Furthermore, although statistical and index-based approaches were applied, the study does not include direct source apportionment or discharge inventory data, limiting definitive identification of pollution sources. The absence of long-term monitoring and ecological response data also restricts a more comprehensive evaluation of ecosystem dynamics.

CONCLUSION

Water quality of the surface water of the Karnaphuli estuary during February 2023 was investigated through the measurement of physiochemical parameters, concentration of various nutrients: phosphate, nitrate, nitrite, ammonia, and silicate, along with chl-*a*. Most measured parameters were within the acceptable limits of the Environmental Conservation Rules (ECR, 2023), although DO showed slightly reduced levels, and ammonia concentrations exceeded the recommended threshold, indicating localized environmental stress. Nutrient concentrations and chl-*a* suggested *moderate* biological activity, which was further reflected in trophic assessments: the NPI indicated generally *qualified* water quality, while TRIX and CTSI consistently pointed to *marginal mesotrophic* conditions, with localized shifts toward eutrophic status at specific stations (notably near Patenga and Parki Beach). Pearson correlation analysis highlighted strong relationships among salinity-driven parameters (salinity, EC, TDS, density), indicating the influence of estuarine mixing, while associations between turbidity, concentration of ammonia, and chl-*a* suggest potential links between suspended matter, nutrient inputs, and phytoplankton dynamics. Exploratory multivariate analyses (PCA and HCA), supported by spatial patterns and land use land cover (LULC) analysis, indicate that stations located near port activities, industrial zones, and urbanized areas exhibit comparatively higher nutrient and turbidity levels. These patterns suggest plausible influences of anthropogenic inputs, including industrial discharge, urban runoff, and port-related activities, although direct causal attribution cannot be confirmed without detailed source-specific measurements or discharge inventories. Overall, the findings highlight emerging nutrient enrichment and spatial heterogeneity in water quality within the KE, emphasizing the need for continuous monitoring, integrated management strategies, and more detailed source-tracking studies to ensure the long-term ecological sustainability of this critical estuarine system.

ACKNOWLEDGEMENT

The authors appreciate the Chemistry and Chemical Oceanography Lab, Bangladesh Maritime University (BMU), for necessary supports.

REFERENCES

Alam, S., Matin, M.A., 2014. Application of 2D morphological model to assess the response of Karnafuli river due to capital dredging. Journal of Water Resources and Ocean Science 2(3), 40-48. https://doi.org/10.11648/j.wros.20130203.13.

Agency for Toxic Substances and Disease Registry, 2004. Toxicological profile for ammonia. Atlanta, GA: U.S. department of health and human services, public health service. https://www.atsdr.cdc.gov/toxprofiles/tp126.pdf.

Ayoade, A. A., Osuala, B. O., Adedapo, T. A., 2019. Physico-chemical parameters, Chlorophyll a and phytoplankton community as trophic state indices of two tropical lakes, southwestern Nigeria. EurAsian Journal of BioSciences 13 (1), 1-8.

Baughman, C. A., Jones, B. M., Bartz, K. K., Young, D. B., Zimmerman, C. E., 2015. Reconstructing turbidity in a glacially influenced lake using the landsat TM and ETM+ surface reflectance climate data record archive, lake clark, Alaska. Remote Sensing, 7, 13692-13710; https://doi.org/10.3390/rs71013692.

Bruce, P., Bruce, A., Gedeck, P., 2020. Practical statistics for data scientists: 50+ essential concepts using R and Python. O'Reilly Media.

Carlson, R. E., 1977. A trophic state index for lakes. Limnology and Oceanography 22(2), 361-369. https://doi.org/10.4319/lo.1977.22.2.0361.

Committee on Environment and Natural Resources (CENR), 2000. An assessment of coastal hypoxia and eutrophication in U.S. waters. National Science and Technology Council.

DoPHE, 2019. Water quality parameter. https://dphe.gov.bd/site/page/15fa0d7b-11f1-45c0-a684-10a543376873/Water-Quality-Parameters-Environment Conservation Rules (ECR), 2023. Surface water quality. Department of Environment.

Geography, GIS, 2021. Inverse distance weighting (IDW) interpolation.

Hawkins, C. P., Norris, R. H., Hogue, J. N., Feminella, J. W., 2000. Development and evaluation of predictive models for measuring the biological integrity of streams. Ecological Applications 10(6), 1456-77. https://doi.org/10.2307/2641298.

Howarth, R. W., Marino, R. M., 2006. Nitrogen as the limiting nutrient for eutrophication in coastal marine ecosystems: Evolving views over 3 decades. Limnology and Oceanography, 51(1, part 2), 364-376. https://doi.org/10.4319/lo.2006.51.1_part_2.0364.

Howladar, M., Chakma, E., Koley, N., Islam, S., Numanbakth, M. A. A., Ahmed, Z., Chowdhury T. R., Akter, S., 2020. The water quality and pollution sources assessment of Surma river, Bangladesh using, hydrochemical, multivariate statistical and water quality index methods, Groundwater for Sustainable Development 12. https://doi.org/10.1016/j.gsd.2020.100523.

Huang, Z., Zheng, S., Liu, Y., Zhao, X., Qiao, X., Liu, C., Zheng, B., Yin, D., 2021. Distribution, toxicity load and risk assessment of dissolved metal in surface and overlying water at the Xiangjaing river in southern China. Sci, Rep.11 (1), 109. https://doi.org/10.1038/s41598-020-80403-0.

Jeffrey, S. W., Humphrey, G. F., 1975. New spectrophotometric equations for determining Chlorophylls a, b, c and C2 in higher plants, algae and natural phytoplankton. Biochemie Und Physiologie Der Pflanzen 167, 191-194. https://doi.org/10.1016/S0015-3796(17)30778-3.

Karim, M., Das, S. K., Paul, S. C., Islam, M. F., Hossain, M. S., 2018. Water quality assessment of Karnaphuli river, Bangladesh using multivariate analysis and pollution indices. Asian Journal of Environment and Ecology 7 (3), 1-11. https://doi.org/10.9734/AJEE/2018/43015.

Mosharraf, A., Begum, F., Dey, M., Rahman, M. M., Susan, M. A. B. H., Akter, F., Sakib, I. A., Hossain, M. A., 2026. Microplastic pollution in the surface water of Karnaphuli estuary: Understanding spatial variation and ecological impacts. Dhaka University Journal of Science 74(1), 36-45. https://doi.org/10.3329/dujs.v74i1.86860.

Nixon, S. W., 1995. Coastal marine eutrophication: A definition, social causes, and future concerns. Ophelia 41, 199-219. https://doi.org/10.1080/00785236.1995.10422044.

Paerl, H. W., 2006. Assessing and managing nutrient-enhanced eutrophication in estuarine and coastal waters: Interactive effects of nitrogen and phosphorus loads. Estuaries and Coasts 29(4), 678-680.

Pettine, M., Casentini, B., Fazi, S., Giovanardi, F., Pagnotta, R., 2007. A revisitation of TRIX for trophic status assessment in the light of the european water framework directive: Application to Italian coastal waters. Marine Pollution Bulletin 54 (9): 1413-1426. https://doi.org/https://doi.org/10.1016.

Rabalais, N. N., Diaz, R. J., Levin, L. A., Turner, R., Rabalais, N. N., Zhang, J., 2010. Dynamics and distribution of natural and human-caused hypoxia. *Biogeosciences 7* (2), 585-619. https://doi.org/10.5194/bg-7-585-2010.

Rezaei, A., Sayadi, M. H., 2014. Long-term evolution of the composition of surface water from the river Gharasoo, Iran: A case study using multivariate statistical techniques. Environ, Geochem, Health 37. https://doi.org/10.1007/s10653-014-9643-2.

Sakib, I. A., Begum, F., Mosharraf, A., Akter, F., Hossain, M. A., Rezwon, S. K. R., Susan, M. A. B. H., 2025. Assessment of pollution and water quality of coastal seawater of Saint Martin's Island. In: Tarekul Islam, G.M., Binte Murshed, S., Haque, S. (eds) sustainable water management and environmental resilience. Springer Water. Springer, Cham. https://doi.org/10.1007/978-3-031-93350-9_3.

Sadi, S. H., Chowdhury, K. M. A., Tasnim, J., Hoque, M. M., Shaheen, M. A. R., Moontahab, A., 2024. Assessing the water quality and its influence on the Chlorophyll-a concentration in the Karnaphuli river estuary. The Dhaka University Journal of Earth and

Environmental Sciences 13(1), 91-104. https://doi.org/10.3329/dujees.v13i1.77579.

Siddique M. A. M., Aktar M., 2012. Heavy metals in salt marsh sediments of porteresia bed along the Karnafully river coast, Chittagong. Soil and Water Research 7, 117-23. https://doi.org/10.1016/j.enmm.2016.01.002.

Smith, V. H., Schindler, D. W., 2009. Eutrophication science: where do we go from here? Trends in Ecology & Evolution 24 (4), 201-207. https://doi.org/10.1016/j.tree.2008.11.009.

Sun, C., Zhen, L., Miah, M. G., 2017. Comparison of the ecosystem services provided by China's Poyang lake wetland and Bangladesh's Tanguar Haor wetland. Ecosystem Services 26, 411-421. https://doi.org/10.1016/j.ecoser.2017.02.010.

Uddin, M. R. Hossain, Md. M., Akter, S., Ali, M. E., Ahsan, Md. A., 2020. Assessment of some physicochemical parameters and determining the corrosive characteristics of the Karnaphuli estuarine water, Chittagong, Bangladesh. Water Science 34(1), 164-180. https://doi.org/10.1080/11104929.2020.1803662.

Vollenweider, R. A., Giovanardi, F., Montanari, G., Rinaldi, A., 1998. Characterization of the trophic conditions of marine coastal waters with special reference to the NW Adriatic Sea: Proposal for a trophic scale, turbidity and generalized water quality index. Environmetrics 9(3): 329-57. https://doi.org/10.1002/(SICI)1099-095X(199805/06)9:3<329::AID-ENV308>3.0.CO;2-9.

Wang, R., Dearing, J. A., Langdon, P., G., Zhang, E., Yang, X., Dakos, V., Scheffer, M., 2012. Flickering gives early warning signals of a critical transition to a eutrophic lake state. Nature 492, 419-422. doi:10.1038/nature11655.

WHO, 2007. The world health report 2007: A safer future: Global public health security in the 21st century. World Health Organization. ISBN: 978-92-4-156344-4.

Zanaga, D., Ruben, K. V. D., Daems, D., De Keersmaecker, W., Brockmann, C., Kirches, G., Wevers, J., Cartus, O., Santoro, M., Fritz, S., Lesiv, M., Herold, M., Tsendbazar, N-E., Xu, P., Ramoino, F., Arino, O., 2022. ESA WorldCover 10 m 2021 v200. https://doi:10.5281/zenodo.7254221.

Zhang, W., Liu, Z., 2021. Daily water quality evaluation of reservoir and cyanobacteria pollution index calculation. Water Science and Technology: Water Supply 21 (2), 836-47. https://doi.org/10.2166/ws.2020.350.